Interplay between Tamm-like and Shockley-like surface states in photonic crystals

N. Malkova*
NASA Ames Research Center, Moffett Field, California 94035, USA

C. Z. Ning†
Center for Nanophotonics, Arizona Institute for NanoElectronics, and Department of Electrical Engineering, Arizona State University, Tempe, Arizona 85287, USA

(Received 1 March 2007; revised manuscript received 31 May 2007; published 5 July 2007)

The goal of this paper is to demonstrate that surface states in a defect chain embedded in a host photonic crystal can be viewed as an interplay between the Tamm-like and Shockley-like states. The defect chain with alternating strong and weak bonds is analyzed using an empirical tight-binding model and the finite difference time domain technique. We investigate how the spectrum of the structures changes with different termination of the chain. It is shown that under certain conditions the Tamm and Shockley states can coexist or can transform from one to the other. These important features allow for controlling the surface states in photonic crystals in frequency, location, and strength.

DOI: 10.1103/PhysRevB.76.045305 PACS number(s): 78.68.+m, 42.70.Qs, 73.20.At, 42.79.Gn

I. INTRODUCTION

There is an increasing interest in surface states in electronic and photonic crystals. As the size of active devices decreases, the role of surfaces becomes increasingly important. Historically, the pioneering papers by Tamm[1] and Shockley[2] marked the beginning of the field of surface physics of solids in the 1930s.[3] Since then, surface states are in general distinguished between Tamm and Shockley states.[3] In the 1970s the first demonstration of the localized photonic surface states in the electromagnetic analog of solids, nowadays called photonic crystals (PCs),[4–6] revealed certain similarities in their properties with those of solids. It was natural to relate the surface states of PCs to the Tamm or Shockley surface states known in solids.[4,6] However, the surface states on PCs often reveal themselves in unexpected ways: for example, in collimating[7–9] and imaging[10] of light. This causes confusion about their properties and their underlying physics.[11,12]

Pursuing a more exact analogy of Tamm's and Shockley's models in PCs recently,[13–15] we investigated the surface states of a one-dimensional defect chain embedded in a host PC. We demonstrated that the Shockley and Tamm surface states indeed have their electromagnetic analogs in PCs. We showed that, in the case of the defect chain with a simple unit cell containing one defect, whenever the surface states appear, they must be the Tamm-like states.[13,15] The Shockley-like surface states appear in a defect chain with a complex unit cell containing two different types of defects and/or strong (short) and weak (long) bonds.[13,14] In this paper we will go beyond the models we studied previously for the pure Schockley[14] or Tamm[15] surface states and consider the possibility of their coexistence.

It is well-known that the Tamm-like and Shockley-like surface states are complementary to each other in the case of solids.[16,17] Both of them are very sensitive to the coupling constants which define the widths of the allowed bands.[3] In Fig. 1 we show the schematic of a one-dimensional atomic chain with the Tamm-like (dashed line) and Shockley-like (solid line) potentials. In Tamm's model[1] the surface states appear entirely due to the perturbation to the potential of the outermost cell of the crystal (surface cell) as shown by the dashed line in Fig. 1. Since the potential of the surface cells is not symmetric with respect to the positions of the surface atoms, the potential is referred to as asymmetric.[2,18] The asymmetry of the surface potential causes the shift (perturbation) of atomic level in the surface cell by a value of Δ with respect to the interior cells as shown in Fig. 1. The perturbation Δ is a key parameter of Tamm's theory. As soon as the value of Δ becomes comparable with the coupling constant, some states fall out of the allowed band into the forbidden band and become the surface states. Therefore the Tamm states are more likely to fall out of the *narrow* allowed band.[15] In contrast, the potential in the surface cell in the case of Shockley's model is similar to that of the interior cells (solid line in Fig. 1), and thus the Shockley-like surface potential is referred to as the symmetric one. Shockley showed that the surface states can appear even in the symmetrical surface potential if the coupling between different atomic orbitals is so strong that they can cross. The Shockley states appear in the so-called inverted band gap formed by anticrossing of the *wide* hybrid bands.[13,15] As a result, there is a narrow window of the widths of the allowed bands where the conditions for both types of the surface states can be satisfied. As a matter of fact this feature is widely used in

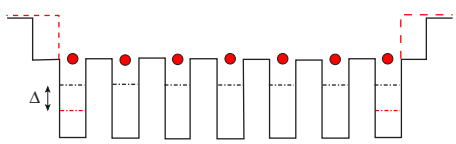

FIG. 1. (Color online) Schematic of one-dimensional atomic chain with the Tamm-like (dashed line) and Shockley-like (solid line) potentials. Δ shows the perturbation of the atomic level (dashed-dotted line) in the surface cell in the case of the Tamm-like potential.

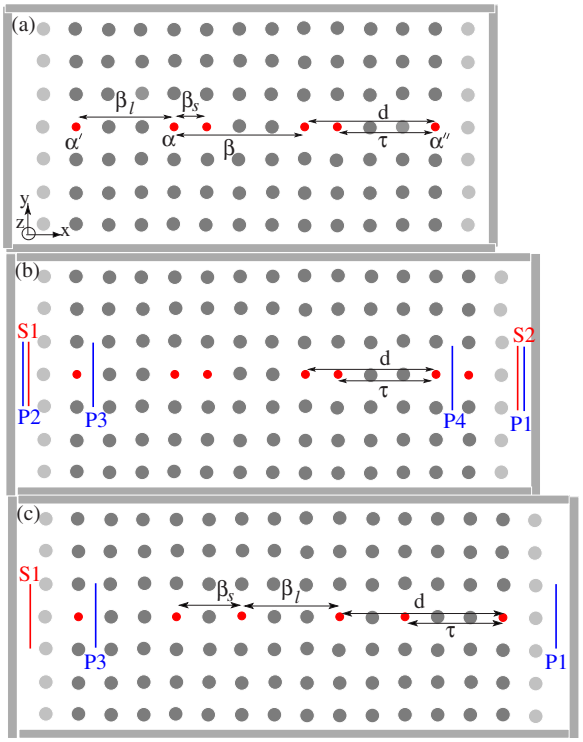

FIG. 2. (Color online) Coupled defect structures with unit cell containing two identical defects (small circles) embedded in a perfect host PC (gray circles). The surface layers of the host crystal shown by light gray circles were removed in order to model the asymmetrical surface potential. The sources (S1 and S2), light collection ports (P1–P4), perfect matched layers (gray boxes), and reference system are shown.

solids. If it is desirable to remove the Shockley-like surface state from the band gap, the surface is passivated by different atoms, which generate the perturbation of the surface potential strong enough to move the surface state into the allowed band.

The goal of this paper is to investigate the correlation between the Tamm-like and Shockley-like surface states on PCs and to demonstrate the possible transformation between them. We consider the Shockley-like states in the presence of an asymmetrical perturbation of the surface potential, which presumably generates the Tamm-like states. We again simplify the problem and study a one-dimensional defect chain embedded in a two-dimensional PC. We focus on the chains of identical defects with alternating strong (short) and weak (long) bonds shown in Fig. 2. We analyze such structures theoretically and numerically using the finite difference time domain (FDTD) simulations to verify empirical tight-binding modeling.[19]

The paper is organized as follows. In Sec. II we describe the model systems to be studied and discuss the tight-binding analysis of the surface states in PCs. In Sec. III, we present the FDTD simulations and explain the numerical results in terms of the tight-binding model. Section IV concludes the paper with a summary of the main results.

II. THEORY OF SHOCKLEY SURFACE STATES OF THE DEFECT CHAIN WITH ASYMMETRICAL SURFACE POTENTIAL

The model systems shown in Fig. 2 represent two-dimensional (2D) arrays of the infinitely long (in the z direction) dielectric rods embedded in another dielectric medium. This otherwise perfect two-dimensional PC (gray circles) is doped with a chain of the defect rods separated by the lattice parameter d. The unit cell of the chain contains two identical defects (small filled circle) supporting the nondegenerate s mode. We design this structure in such a way that the chain would generate the defect states (or the allowed band of the chain) inside the band gap of the host crystal. Then in the first-order approximation, we neglect the coupling between the defect rods and the host crystal. Therefore we can consider this structure as a periodic chain installed in another quasihomogeneous medium, whose role is to confine light in the direction perpendicular to the chain and to generate defect states of desired type. We consider three structures: structures 1 and 3 with complete unit cells [Figs. 2(a) and 2(c)] and structure 2 with incomplete unit cells [Fig. 2(b)]. For all structures, we distinguish two cases of the surface potential. It was shown[15] that the perturbation of the end defect of the chain strongly depends on its separation from the surface of the host PC. The surface unit cell is only perturbed when the end defects of the chain are placed on the surface of the host crystal. Thus we create a perturbed surface cell by removing the surface layers of the host crystal shown in light gray circles in Figs. 2(a) and 2(b) (compare with dashed line in Fig. 1).

For theoretical analysis, we use the tight-binding approach described in detail in Refs. 13 and 14. We briefly specify the model for the structures studied in this paper. The defect chains in Fig. 2 include N unit cells separated by the lattice parameter d. Each unit cell of the chain (Fig. 2) contains two s defects shifted with respect to each other by τ. The wave function of the chain is expressed as a linear combination of the s-type eigenmodes, $\phi_s(r-nd)$ and $\phi_s(r-\tau-nd)$, of the individual defects of the nth unit cell $\Psi(r,t)=\Sigma_{n=1}^{N}[a_n(t)\phi_s(r-nd)+b_n(t)\phi_s(r-\tau-nd)]$. The dynamics of the field amplitudes $a_n(t)$ and $b_n(t)$ is described by the following set of ordinary differential equations:[14]

$$i\frac{d}{dt}a_n = \alpha a_n + \beta(a_{n-1} + a_{n+1}) + \beta_l b_n + \beta_s b_{n-1},$$

$$i\frac{d}{dt}b_n = \alpha b_n + \beta(b_{n-1} + b_{n+1}) + \beta_l a_n + \beta_s a_{n+1}, \qquad (1)$$

where $\alpha=\omega-i\gamma$ are the complex eigenvalues of the individual s defects defined by the frequency, ω, and by the width, γ, of the resonant peak. The coupling matrix elements β, β_l, and β_s are overlap integrals between the relevant defect modes as specified in Fig. 2(a). The β defines the coupling between the identical defects in the closest unit cells, with the value of 4β being the width of the allowed band

forthe chain with one defect in the unit cell. The β_s and $\beta_l$define the coupling through the short and long bonds, respectively.

For an infinite chain of the defects, the solution of problem (1) gives the dispersion relation:

$$\omega_{1,2}(k) = \alpha + 2\beta\cos(kd) \pm \beta_{ls}, \tag{2}$$

where $\beta_{ls}^2 = \beta_s^2 + \beta_l^2 + 2\beta_s\beta_l\cos(kd)$. The two branches of the spectrum $\omega_{1,2}$ describe the so-called bonding and antibonding bands.

For a finite chain, we consider the case when the chain is terminated by the strong (short) bonds and the Shockley surface states can appear.[13] For a chain of N unit cells we obtain the following eigenvalue problem:

$$\begin{pmatrix}
\alpha'-\omega & \beta_s' & \beta' & 0 & 0 & 0 & \cdots & 0 & 0 & 0 & 0 \\
\beta_s' & \alpha-\omega & \beta_l & \beta & 0 & 0 & \cdots & 0 & 0 & 0 & 0 \\
\beta' & \beta_l & \alpha-\omega & \beta_s & \beta & 0 & \cdots & 0 & 0 & 0 & 0 \\
0 & \beta & \beta_s & \alpha-\omega & \beta_l & \beta & \cdots & 0 & 0 & 0 & 0 \\
\vdots & \vdots & \vdots & \vdots & \vdots & \vdots & \vdots & \vdots & \vdots & \vdots & \vdots \\
0 & 0 & 0 & 0 & 0 & 0 & \cdots & \beta & \beta_l & \alpha-\omega & \beta_s'' \\
0 & 0 & 0 & 0 & 0 & 0 & \cdots & 0 & \beta'' & \beta_s'' & \alpha''-\omega
\end{pmatrix}
\begin{pmatrix}
A_1 \\ B_1 \\ A_2 \\ B_2 \\ \vdots \\ A_N \\ B_N
\end{pmatrix} = 0. \tag{3}$$

Here we introduce the asymmetry of the surface potential through the perturbation of the eigenvalues (α' and α'') and coupling constants (β', β'', β_s', and β_s'') of the end defects. The solution of Eq. (3) defines $2N$ eigenenergies, ω_n, and eigenfunctions, Ψ_n, with $|\Psi_n|^2 = \Sigma_{i=1:N}(A_{in}^2 + B_{in}^2)$.

First we analyze the eigenvalue problem (3) for structure 1 or 3 with four complete unit cells [Figs. 1(a) and 1(c)] when we gradually increase the perturbation of the end defects. For simplicity we assume that the surface perturbation does not affect the coupling constants ($\beta' = \beta'' = \beta$ and $\beta_s' = \beta_s'' = \beta_s$). First we consider the case when both end defects are perturbed identically ($\alpha' = \alpha'' \neq \alpha$). We describe the surface perturbation by the dimensionless parameter $\Delta = (\alpha - \alpha')/\beta_l$ and use the dimensionless units for energy, $(\omega - \alpha)/\beta_l$. Since the $\beta_{l,s}$ describe the coupling between the nearest neighbors and the β describes the coupling between the next nearest neighbors, we can assume that $\beta_{l,s} \gg \beta$.

As shown in Ref. 13, for the structure with alternating short and long bonds the governing parameter for the surface states is the ratio of strengths of the bonds, $\eta = \beta_s/\beta_l$. As soon as $\eta > 1$ the surface states appear at the edges of the allowed bands, and they move deeper inside the band gap when η increases. We demonstrate the solution of eigenvalue problem (3) for the chain of four complete unit cells at $\Delta = 0$ and 4.5 in Figs. 3(a) and 3(b) and Figs. 3(c) and 3(d), respectively. We assumed here that $\eta = 3$. The eigenvalues are shown by the stars and the dispersion relation of infinite chain calculated from Eq. (2) is shown by the solid lines in Figs. 3(a) and 3(c). The corresponding absolute values of wave functions $|\Psi|$ defined above are presented in ascending order from bottom to top in Figs. 3(b) and 3(d). Figure 3(e) demonstrates the change of the energy levels of the chain as a function of perturbation Δ. The dashed regions show the allowed bands of infinite chain.

We can see from Fig. 3(a) that at $\Delta = 0$ the two states fall out of the allowed bands. They form the two surface states almost in the middle of the band gap. These states are characterized by the imaginary value of k and strongly localized at the surface [see Fig. 3(b)]. Since these states are caused by the termination of the chain by the strong bonds, they are the Shockley surface states. With increasing in perturbation Δ, these states move down in energy [see Fig. 3(e)]. At $\Delta \sim 3$ they reach band-edge of the lower allowed band and become conducting states characterized by the real value of momentum k. Simultaneously, at $\Delta > 3$ two other states fall out of the lower allowed band and form the surface states [see Figs. 3(c) and 3(d)]. Such surface states must be classified as the Tamm states because they are caused by the perturbation of the surface potential. Importantly, the condition $\Delta > 3$ implies that the perturbation Δ becomes as large as the η parameter. We therefore see that the Shockley surface states can transform into the Tamm surface states when the perturbation of the surface cell becomes as large as the ratio of strengths of the bonds, $\Delta > \eta$.

From Fig. 3(e) we also note that the two Shockley surface states deep inside the band gap almost overlap each other. These states can be split into two well-separated states, for example, if only one of the end defects is perturbed ($\alpha' \neq \alpha'' = \alpha$). Figure 3(f) shows the energy levels versus the perturbation Δ when only one of the end defects is perturbed in contrast to Fig. 3(e) when both end defects are perturbed. We can see that with increasing perturbation only one of the Shockley states moves down in energy and finally converts into the Tamm state at $\Delta > \eta$. The other state stays unchanged through the entire interval of the Δ. In the interval $0 < \Delta < \eta$ the separation between the two states is proportional to the perturbation Δ. It is interesting to note that this structure gives a wonderful example of the coexistence of the

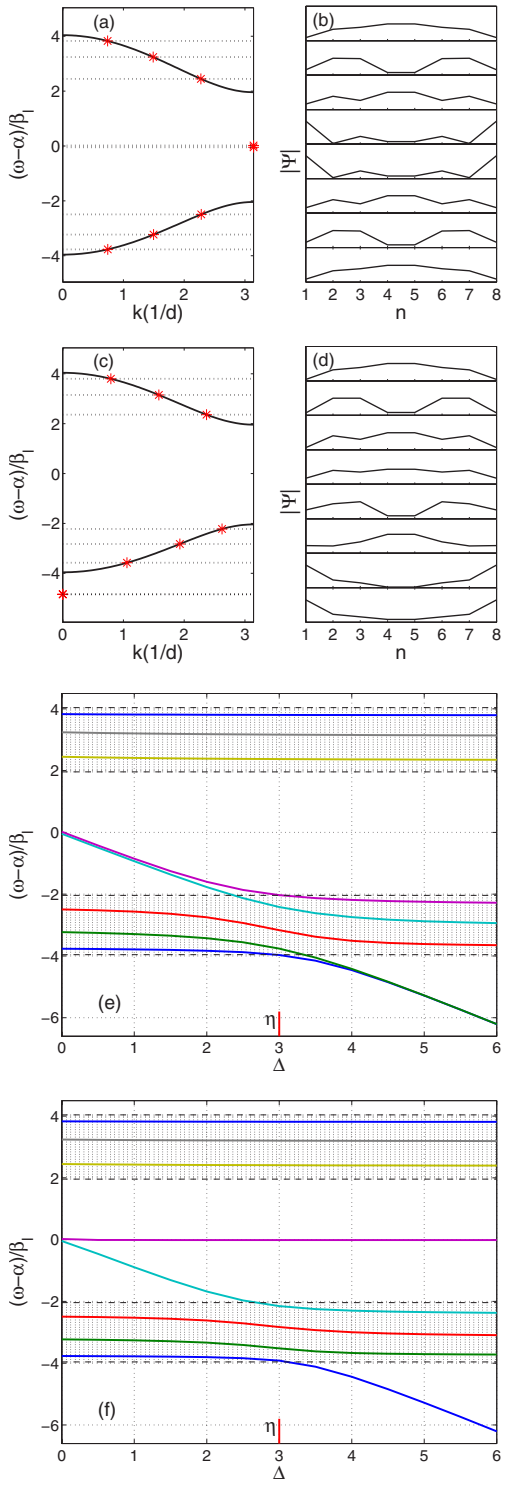

FIG. 3. (Color online) The solution of eigenvalue problem (3) for the chain of four complete unit cells at $\Delta=0$ [(a) and (b)] and $\Delta=4.5$ [(c) and (d)]. The eigenvalues are shown by stars and the dispersion relations of infinite chain calculated from Eq. (2) are shown by solid lines in (a) and (c). The corresponding absolute values of the wave functions $|\Psi|$ are presented in ascending order from bottom to top in (b) and (d). The change of the energy levels of the chain as a function of the perturbation Δ is demonstrated in (e) when both end defects are perturbed and in (f) when only one end defect is perturbed. The dashed regions show the allowed bands of infinite chain.

Tamm and Shockley surface states on the two sides of the sample.

Figure 4 shows the solution of the eigenvalue problem for structure 2 [Fig. 2(b)], which represents a defect chain of five incomplete cells. The spectrum and the wave functions at $\Delta=0$, 2, and 4.5 are shown in Figs. 4(a) and 4(b), Figs. 4(c) and 4(d) and Figs. 4(e) and 4(f), respectively. The change of the energy levels versus the perturbation parameter Δ is demonstrated in Fig. 4(g).

As we discussed in Ref. 13 in the nonperturbed case, any structure with alternating strong and weak bonds with incomplete unit cells has one Shockley surface state almost in the middle of the inverted band gap [see Fig. 4(a)]. This state is localized at the defect with the strong broken bond as shown in Fig. 4(b). We can see in Fig. 4(g) that with increasing perturbation, this state moves down in energy and, simultaneously, the two states fall out of the allowed bands at $\Delta > 1$. They form the surface states on the opposite side of the chain with the weak broken bond [see the first and sixth from the bottom curves in Fig. 4(f)]. These states are caused by the surface perturbation and, therefore, are the Tamm surface states. We can see in Fig. 4(g) that at $1<\Delta<\eta$ the Shockley and Tamm surface states coexist. Finally at $\Delta>\eta$, the Shockley state merges with the lower allowed band and the Tamm-like surface state falls from the lower allowed band [see Figs. 4(e) and 4(f)]. We can view this effect as transition or conversion of the Shockley state into the Tamm state even so there is no continuous transition between those states in terms of energy; but both the Tamm and Shockley states are caused by the termination of the chain, being localized on the surface.

From this analysis we conclude that, by varying the perturbation of the surface potential, the surface states can be converted from the Shockley-like into Tamm-like surface states. Critical condition for this conversion is that the perturbation of the surface cell must be larger than the ratio of strengths of the bonds. We have also seen that for the structure with incomplete unit cells the Tamm-like and Shockley-like surface states can coexist in the interval $1<\Delta<\eta$.

III. NUMERICAL RESULTS

Next we will conduct numerical simulations to confirm the theoretical analysis presented in the last section. For the numerical investigation we use the FDTD technique.[20] Our computational domain is shown in Fig. 2. It was divided into uniform square mesh $\Delta x=a/40$ (a is the lattice constant of the host crystal). The computational domain was surrounded by perfectly matched layers (gray boxes in Fig. 2), with the thickness corresponding to ten layers of the discretization grid. The numerical simulations were performed with a total of 100 000 time steps, with each time step $\Delta t=\Delta x/(2c)$. In order to excite the surface states on both sides of the chain, we examined the structures in two runs. At first by launching a Gaussian beam at one side of the structure (S1 in Fig. 2) we analyzed the transmission and near field spectrum by collecting the signal at ports P1 and P3, respectively. In the second run, we launched the beam at the other side (S2 in Fig. 2) and collected the signal at ports P2 and P4. The transmission

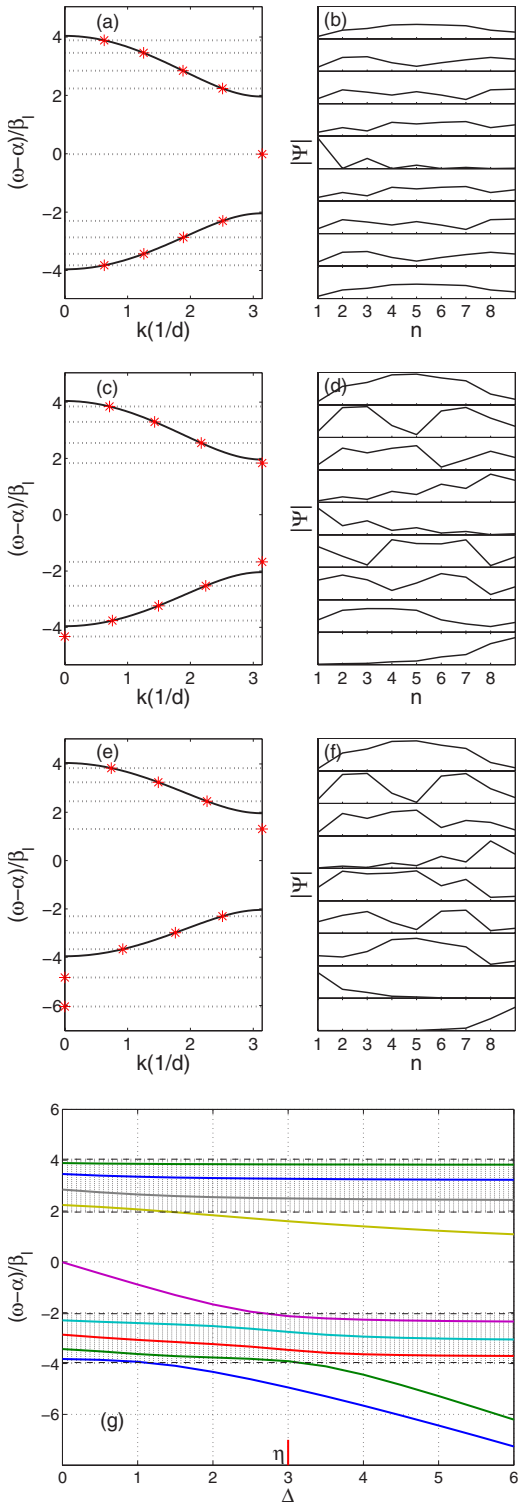

FIG. 4. (Color online) The solution of eigenvalue problem (3) for the chain of five incomplete unit cells at $\Delta=0$ [(a) and (b)], 2 [(c) and (d)], and 4.5 [(e) and (f)]. The eigenvalues are shown by stars and the dispersion relation of infinite chain calculated from Eq. (2) are shown by solid lines in (a), (c), and (e). The corresponding absolute values of the wave functions are presented in ascending order from bottom to top in (b), (d), and (f). The change of the energy levels of the chain as a function of the perturbation Δ is demonstrated in (g). The dashed regions show the allowed bands of infinite chain.

coefficient was calculated by normalizing the collected signal or response function at Ports 1 and 2 to the reference signal. The spatial width of the beam was equal to 20 grid cells. A frequency spectrum of the source covered the region of interest $\Delta\tilde{\omega}=0-0.4$.

Our choice of the structure to demonstrate the effect of the surface perturbation on the Shockley states must satisfy two main requirements: (1) a weak coupling between the allowed bands of the host crystal and defects; and (2) a large perturbation of the end defects. The first requirement can be satisfied if the relevant band gap of the host PC is much larger than the width of the allowed bands of the defect chain. Therefore we chose the defect chain with sufficiently large lattice parameter ($d=4a$ for structures 1 and 2). As for the second requirement, we know that the perturbation of the end defect can be controlled by its separation from the surface of the host PC.[15] The perturbation is at maximum when the end defect of the chain is placed at the surface of the host PC, and it is decreasing fast when the end defect moves away from the surface of the crystal. Our analysis showed that in the case of the square lattice of the silicon rods ($\epsilon_r=11.9$) in vacuum, the strongest perturbation is achieved for the defect rods of $R_d=0.18a$ embedded into the host crystal with $R=0.35a$.

The results of our analysis for structures 1 and 2 are shown in Figs. 5 and 6, respectively. The transmission coefficients for these structures are presented in Figs. 5(a) and 6(a), respectively. The solid lines show the data for the case of perturbed end defects and the dashed lines correspond to the structures with nonperturbed defects. We can clearly see the shift of the central peak corresponding to the Shockley state in the perturbed structure. The distributions of $|E_z|$ for these modes are presented in Figs. 5(d) and 6(d).

We analyze the transmission coefficient of structure 1 with complete unit cells in Fig. 5(a). We assume that the central peak corresponds to the overlapping of the two close peaks as predicted by theory [see Fig. 3(e)]. Thus the number of peaks in the transmission spectrum is equal to the number of defects in the chain. In accordance with the theory, the distributions of the fields in the allowed bands of the defect chain are described by the bonding [Fig. 5(e)] and antibonding [Fig. 5(c)] orbitals. We conclude that in the case of structure 1 with complete unit cells the perturbation of the surface unit cell does not give rise to other surface state but shifts the Shockley surface state down in energy.

In contrast, in the case of perturbed structure 2 with incomplete unit cells, the number of peaks in the transmission spectrum is two less than the number of defects [compare solid and dashed lines in Fig. 6(a)]. In order to identify all the states we analyzed the response function at ports P3 and P4 [see Fig. 2(b)] as described above. In Fig. 6(f) we show the response functions at ports P3 (dashed line) and P4 (dash-dotted line) along with transmission coefficient at port P1 (solid line). First of all we note that the response function at port P3 confirms the existence of the Shockley surface state as a weak peak in the transmission spectrum [compare solid and dashed lines in Fig. 6(f)]. Second, the response function at port P4 clearly shows the two surface states close to the band edges of the allowed bands. These states are caused by the perturbation of the surface cell, therefore they

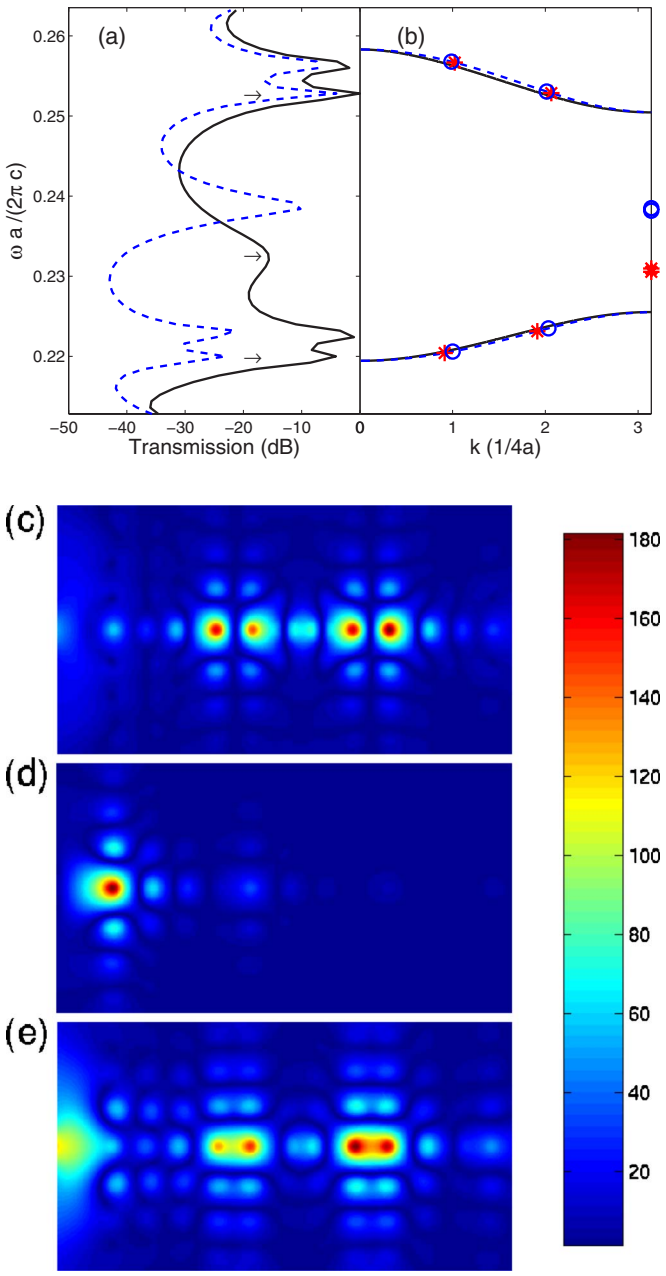

FIG. 5. (Color online) Structure 1 with three complete unit cells: (a) Calculated transmission coefficient for the case of perturbed (solid line) and nonperturbed (dashed line) end defects. (b) Theoretical dispersion relationship: The solid and dashed lines represent the supercell plane wave calculation and fitted dispersion relation $\omega_{1,2}(k)$ [Eq. (2)] for the infinite chain, respectively. The stars and circles show the calculated spectrum of the finite chains with perturbed and nonperturbed end defects, respectively. The $|E_z|$ distributions for the modes pointed out by arrows in (a) are presented in descending order from top to bottom in (c)–(e).

are the Tamm surface states. The field distributions of these states are shown in Figs. 6(c) and 6(e). In agreement with the theoretical predictions, these states are localized on the opposite side of the Shockley surface state [compare Figs. 4(c) and 4(d) and Figs. 6(c)–6(e)].

In order to study the underlying physics of the surface states studied, we analyze the results of the FDTD simulations in terms of the tight-binding model discussed in Sec. II. This empirical model contains parameters, α, β, and $\beta_{s,l}$. We found these parameters by fitting the dispersion relation Eq. (2) with the exact (*ab initio*) spectrum of the infinite defect chain embedded into the host crystal calculated by means of the supercell plane-wave technique. According to dispersion relation for the infinite chain Eq. (2), the band gaps at $kd=0$ and π are defined as $\epsilon_g^{0,\pi}/\beta_l=2(\eta\pm1)$, the widths of the allowed bands are equal to $\Delta\epsilon_{1,2}=|4\beta\pm2\beta_l|$. Thus the spectrum of infinite chain at $kd=0$ and π completely defines unknown parameters of the nonperturbed structure. Using the supercell plane-wave technique, we found the spectrum of the infinite chain and estimated the parameters for structures 1 and 2 as follows: $\eta=\beta_s/\beta_l=4.57$, $\beta=0.057\beta_l$. In the case of the perturbed structure, we also have to take into account the perturbation of the end defects Δ. We found the value of Δ as was described in Ref. 15 from the FDTD numerical analysis. For the structure studied we estimate that $\Delta\beta_l=2.28(1+0.3i)$. It is important to note that due to a strong decay of the defect mode at the ends of the chain, the value of Δ is complex.[15] We can see that $|\Delta|<\eta$ for structures 1 and 2.

Using the parameters, we calculated the spectrum of the finite chain. The results of our analysis are summarized in Figs. 5(b) and 6(b). The solid lines present the supercell plane-wave calculation of the spectrum for the infinite chain. The dashed curves show dispersion relation Eq. (2) for the infinite chain. The stars show the discrete spectrum of the finite chain calculated from Eq. (3). The theoretical analysis clearly demonstrates the two close surface states inside the band gap for the structure with complete unit cells. These states are characterized by the complex wave vector $k=\pi\pm i\kappa$. In the case of a structure with complete unit cells $\kappa\sim1.3/d$, which agrees very well with the localization length of the surface modes, $l_s\sim1/\kappa\sim0.8d$ [see Fig. 5(d)].

Next we analyze structure 1 when only one of the end defects is perturbed. This case corresponds to the structure shown in Fig. 2(a) with right or left surface layers (light gray circles) removed. We present in Fig. 7(a) the transmission coefficient of this structure (solid lines) along with the response functions at ports P3 (dashed line) and P4 (dash-dotted line). As described above we have also performed the theoretical modeling of the structure, which is shown in Fig. 7(b). In agreement with the theoretical prediction [Fig. 7(b)] we can clearly see the splitting of the central peak into the two states in Fig. 7(a). The distributions of $|E_z|$ for these modes presented in Figs. 7(c) and 7(d) show that these states are located on the different sides of the chain.

It follows from our estimates for the structures studied before that $\Delta<\eta$. Therefore for these structures, we cannot observe the transformation from the Shockley states into the Tamm states discussed in Sec. II. How could we design the structure in order to have $\Delta>\eta$ required for this transition? We know that in the tight-binding model[19] the coupling constants are inversely proportional to the separation between the defects. Recalling definition of the parameters $\Delta=(\alpha-\alpha')/\beta_l$ and $\eta=\beta_s/\beta_l$, we conclude that, given the value of surface perturbation $\alpha-\alpha'$, we can meet the criteria for the transition by increasing the length of the short bond. On the

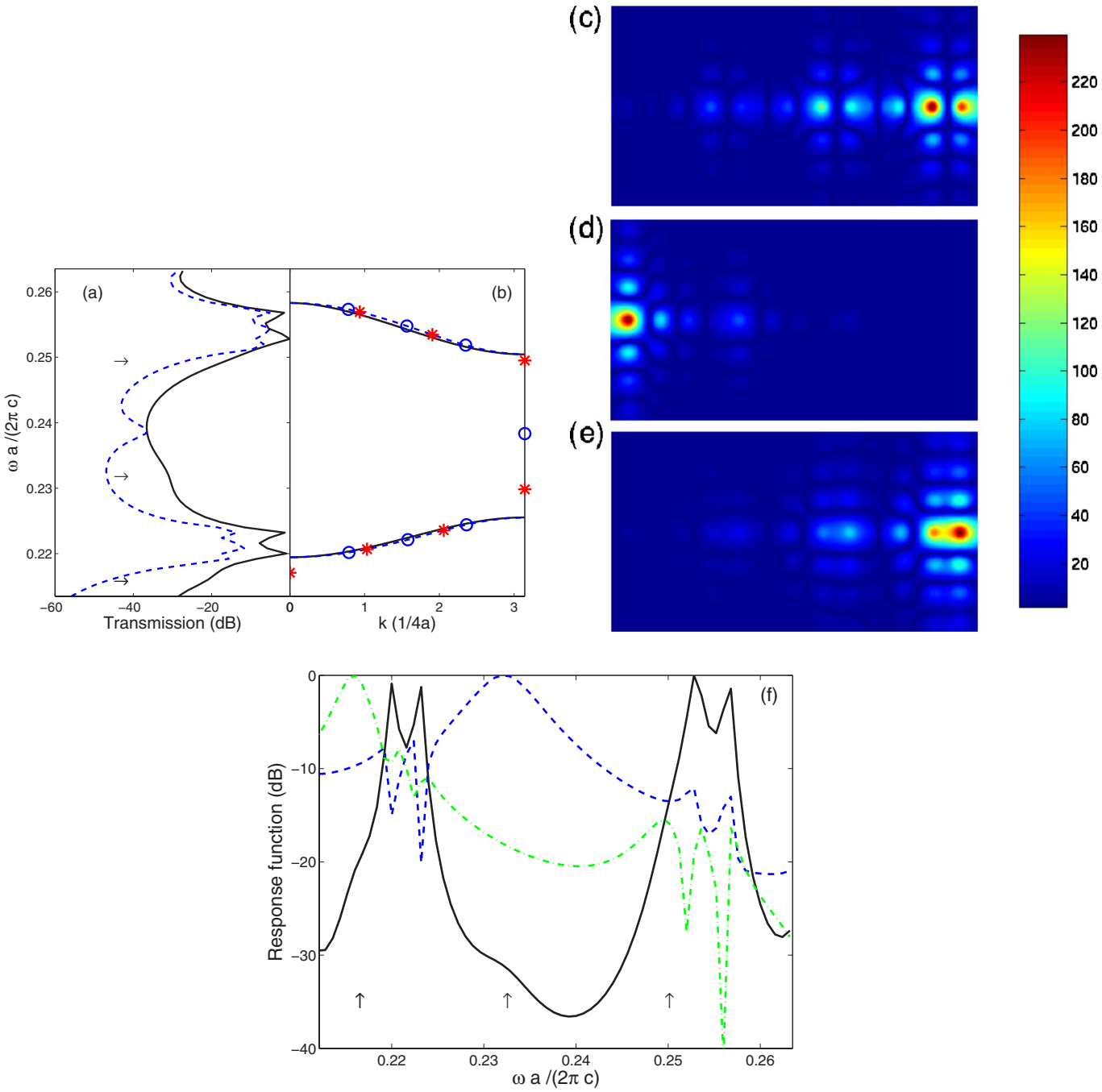

FIG. 6. (Color online) Structure 1 of four incomplete unit cells. (a) Calculated transmission coefficient for the case of perturbed (solid line) and nonperturbed (dashed line) end defects, where the arrows indicate the surface modes. (b) Theoretical dispersion relationship: The solid and dashed lines represent the supercell plane wave calculation and fitted dispersion relation $\omega_{1,2}(k)$ [Eq. (2)] for the infinite chain, respectively. The stars and circles show the calculated spectrum of the finite chains with perturbed and nonperturbed end defects, respectively. The $|E_z|$ distributions for the modes pointed out by arrows in (a) are presented in descending order from top to bottom in (c)–(e). The response functions at ports P3 (dashed line) and P4 (dash-dotted line) along with transmission coefficients at ports P1 and P2 (solid line) are shown in (f). The arrows indicate the surface modes.

other hand, the existence of the Shockley states requires $\eta > 1$. Therefore in order to meet all the requirements we have to increase the length of the short bond, while keeping the length of the long bond unchanged. We finally come to structure 3 with period $d=5a$ shown in Fig. 2(c).

Figure 8(a) shows the transmission coefficient (solid line) and response function at port P3 (dash-dotted line) for structure 3 in the case of perturbed surface cells in comparison with the transmission coefficient in the case of nonperturbed surface cells (dashed line). The theoretical modeling of this structure is presented in Fig. 8(b), where stars and circles show the discrete spectrum of the finite perturbed and nonperturbed chains, respectively. We can see that in the absence of surface perturbation, the two close-by Shockley-like sur-

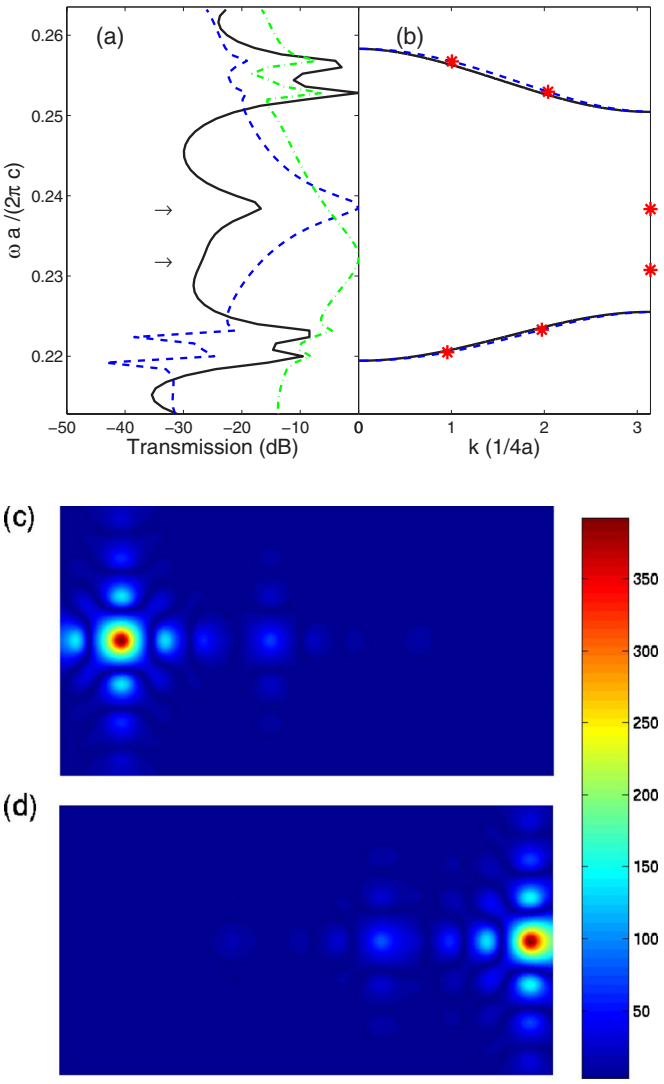

FIG. 7. (Color online) Structure 1 with three complete unit cells when only one of the end defects was perturbed. (a) Calculated transmission coefficient (solid line) and response functions at ports P3 (dashed line) and P4 (dash-dotted line). The arrows indicate the surface modes. (b) Theoretical dispersion relationship: all notations are similar to Fig. 5(b). The $|E_z|$ distributions for the modes pointed out by arrows in (a) are presented in descending order from top to bottom in (c) and (d).

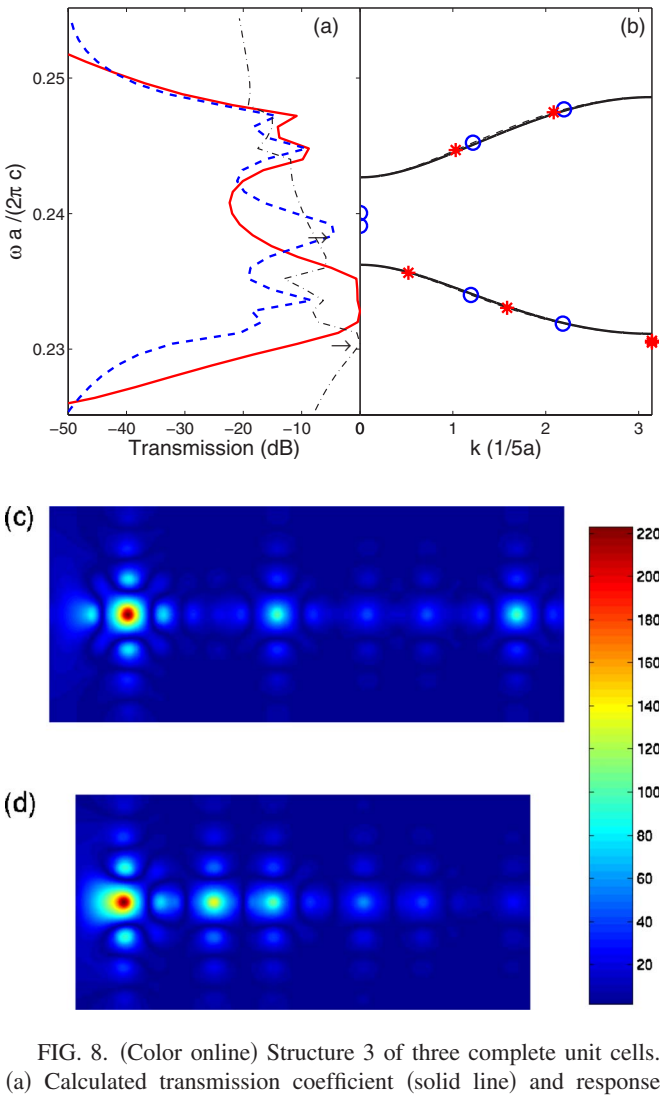

FIG. 8. (Color online) Structure 3 of three complete unit cells. (a) Calculated transmission coefficient (solid line) and response functions at port P3 (dash-dotted line) in the case of perturbed surface cells in comparison with the transmission coefficient in the case of nonperturbed surface cells (dashed line). The arrows indicate the surface modes. (b) Theoretical dispersion relationship. The solid and dashed lines represent the supercell plane wave calculation and fitted dispersion relation $\omega_{1,2}(k)$ [Eq. (2)] for the infinite chain, respectively. The stars and circles show the discrete spectrum of the finite perturbed and nonperturbed chains, respectively. The $|E_z|$ distributions for the surface modes pointed out by arrows in (a) for the structure with nonperturbed (c) and perturbed (d) surface cells.

face states appear almost in the middle of the inverted band gap. The field distribution for these states is shown in Fig. 8(c). In the case of perturbed surface cells, these states transform into the Tamm-like surface states and fall out of the lower allowed band. The field distribution for these states is shown in Fig. 8(d). We can see that the Shockley-like surface states are well-defined even in the transmission spectrum. When these states transform into the Tamm-like states, they can be hardly identified from the transmission experiment only, the near-field measurements must be used in addition.

We finally note that in all structures studied in this paper, the existence of the surface states deeply inside the band gap considerably reduces the transmission of the structure. As soon as the surface state approaches the allowed band, the transmission of the structures increases considerably [see dashed and solid lines in Figs. 5, 6, and 8(a)]. This data is consistent with the published results on enhancement of the transmission of the PC waveguide via the surface states.[8] In terms of the model developed we explain this effect as follows. The coupling of the surface states to the allowed states can facilitate the transmission through the structure. When the surface state moves far away from the allowed states so that they cannot efficiently couple with each other, the surface state traps the light at the surface and reduces the transmission. Remarkably, this effect immediately follows from Eq. (6) for the transmission coefficient derived in Ref. 15.

IV. CONCLUSION

We investigated the effect of the perturbation of the end defects on the Shockley-like surface states of the defect chains embedded in a host PC. We studied the structures with complete and incomplete unit cells. We found that the perturbation of the end defects affects the Shockley surface states differently in these cases. In the case of complete unit cells, the two close surface states move simultaneously down in energy if both end defects are equally perturbed. They convert into the Tamm-like surface states when $\Delta > \eta$. If only one of the end defects is perturbed, one of the surface states moves down in energy and another one remains unchanged. The separation between these states is proportional to the value of Δ. The split state converts into the Tamm-like surface state for $\Delta > \eta$. The situation is different for the structure with incomplete unit cells. In this case one Shockley-like surface state moves down in energy and converts into the Tamm-like state for $\Delta > \eta$. In addition, the two Tamm-like surface states fall out of allowed bands when $\Delta > 1$, so that the Tamm-like and Shockley-like surface states can coexist when $1 < \Delta < \eta$. Importantly, the Shockley states are always associated with the strong broken bond, while the Tamm states with the weak one. We conclude that the nature of surface states strongly depends on the surface boundary conditions. Given the symmetry of the infinite structure and the boundary conditions, the character of the surface states is completely defined by the strengths of bonds terminating the structure.

In this paper we investigated the effect of the perturbation of the end defects caused by the natural conditions on the surface of the host PC. The theoretical results reported are important in their own right for the relevant waveguide devices. Besides this, we believe that the effect of the perturbation induced by the external forces, for example, the change of the radii or dielectric constant of the end defects or the symmetry of the surrounding rods of the host PC, can be successfully exploited in surface sensor devices. A preliminary analysis gives that the required changes in radius and dielectric constant must be about 1%–5%. However, more detail analysis of the dependence of coupling constants from the dielectric constant and radius of the defects is needed to give a more precise estimation.

*nmalkova@hotmail.com
†cning@asu.edu

[1] I. E. Tamm, Phys. Z. Sowjetunion **1**, 733 (1933); Z. Phys. **76**, 849 (1932).
[2] W. Shockley, Phys. Rev. **56**, 317 (1939).
[3] A. Many, Y. Goldstein, and N. B. Grover, *Semiconductor Surfaces* (North-Holand, Amsterdam, 1965); S. G. Davison and M. Stesliska, *Basic Theory of Surface States* (Oxford University Press, Oxford, 1992).
[4] P. Yeh, A. Yariv, and C.-S. Hong, J. Opt. Soc. Am. **67**, 423 (1977).
[5] J. A. Arnaud and A. A. M. Saleh, Appl. Opt. **13**, 2343 (1974).
[6] P. Yeh and A. Yariv, Appl. Phys. Lett. **32**, 104 (1978).
[7] P. Kramper, M. Agio, C. M. Soukoulis, A. Birner, F. Muller, R. B. Wehrspohn, U. Gosele, and V. Sandoghdar, Phys. Rev. Lett. **92**, 113903 (2004).
[8] E. Moreno, F. J. Garcia-Vidal, and L. Martin-Moreno, Phys. Rev. B **69**, 121402(R) (2004).
[9] S. K. Morrison and Y. S. Kivshar, Appl. Phys. Lett. **86**, 081110 (2005).
[10] X. Wang and K. Kempa, Phys. Rev. B **71**, 085101 (2005).
[11] B. Wang, W. Dai, A. Fang, L. Zhang, G. Tuttle, Th. Koschny, and C. M. Soukoulis, Phys. Rev. B **74**, 195104 (2006).
[12] R. Moussa, Th. Koschny, and C. M. Soukoulis, Phys. Rev. B **74**, 115111 (2006).
[13] N. Malkova and C. Z. Ning, Phys. Rev. B **73**, 113113 (2006).
[14] N. Malkova and C. Z. Ning, J. Opt. Soc. Am. B **24**, 707 (2007).
[15] N. Malkova and C. Z. Ning, J. Phys.: Condens. Matter **19**, 056004 (2007).
[16] J. Klos and H. Puszkarski, Phys. Rev. B **68**, 045316 (2003).
[17] E. Foo and H. Wong, Phys. Rev. B **9**, 1857 (1974).
[18] J. Zak, Phys. Rev. B **32**, 2218 (1985).
[19] E. Lidorikis, M. M. Sigalas, E. N. Economou, and C. M. Soukoulis, Phys. Rev. Lett. **81**, 1405 (1998).
[20] A. Taflove and S. C. Hagness, *Computational Electrodynamics: The Finite Difference Time Domain Method* (Artech House, Boston, 2000).